JOC The Journal of Organic Chemistry

Article

pubs.acs.org/joc

# Tethered 1,2-Si-Group Migrations in Radical-Mediated Ring Enlargements of Cyclic Alkoxysilanes: An EPR Spectroscopic and Computational Investigation

John C. Walton,*[,†] Ryutaro Kanada,[‡] Takeaki Iwamoto,[§] Satoshi Shuto,[‡] and Hiroshi Abe*[,∥]

[†]EaStCHEM School of Chemistry, University of St. Andrews, St. Andrews, Fife, KY16 9ST, U.K.

[‡]Graduate School of Pharmaceutical Sciences, Hokkaido University, Kita-12, Nishi-6, Kita-ku, Sapporo 060-0812, Japan

[§]Department of Chemistry, Graduate School of Science, Tohoku University, 980-8578 Sendai, Japan

[∥]Department of Chemistry, Graduate School of Science, Nagoya University, Furo, Chikusa, Nagoya 464-8602, Japan

Supporting Information

**ABSTRACT:** 5- to 6-member ring enlargements of 3-oxa-2-silacyclopentylmethyl to 4-oxa-3-silacyclohexyl radicals were investigated by EPR spectroscopy and QM computations of model indano-oxasilacyclopentane and oxasilinanyl compounds. Both experimental and computational evidence favored a mechanism via a concerted 1,2-migration of the "tethered" Si-group. Thus, the "forbidden" 1,2-Si-group migration from carbon to carbon becomes allowed when the Si-group is "tethered". The EPR data from 3-oxa-2-silacyclopentylmethyl radicals disclosed ground state conformations having semioccupied p-orbitals close to *antiperiplanar* with respect to their *β*-Si−C bonds, but indicated Si-hyperconjugation (*β*-silicon effect) was insignificant in radicals. Kinetic data was obtained by the steady state EPR method for ring enlargement of indano-3-oxa-2-silacyclopentylmethyl radicals. The scope of the novel rearrangement in terms of other ring types and sizes, as well as the analogous 1,2-migration of "tethered" C-centered groups, was explored computationally.

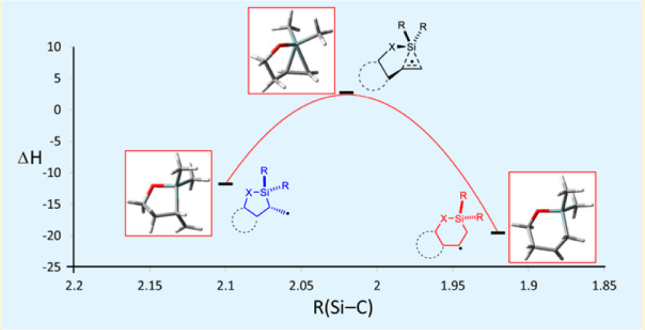


## INTRODUCTION

Vinylsilyl ethers are easily prepared by treatment of alcohols with vinylsilyl chlorides and are versatile and effective reagents for organic syntheses. In particular, this moiety has been introduced to numerous alcohol types as a temporary tether with radical acceptor potential.[1] When the alcohol segment contains a substituent *β*-to the oxygen atom, that is suitable as a leaving group for radical generation (**1**, Scheme 1), then homolytic ring closure affords cyclic alkoxysilanes.[2] The latter readily yield diols when oxidatively ring-opened with fluoride under Tamao conditions.[3,4] This sequence has been exploited in successful preparations of branched nucleosides[5] and C-glycosides.[6,7]

**Scheme 1. Preparation of 5- and 6-Member Ring Alkoxysilanes**

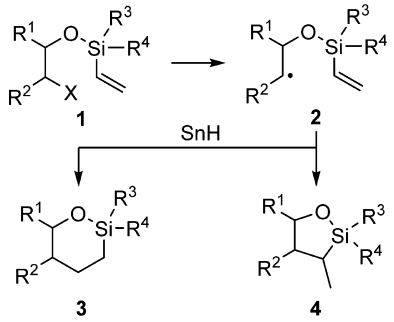


Intriguing examples of the process were discovered in which *either* 6- *or* 5-member ring alkoxysilanes (**3** or **4**) could be isolated, depending on reaction conditions.[8] Initially it seemed that ring formation might involve 6-*endo*- or 5-*exo*- cyclizations of intermediate C-centered radical **2** (Scheme 1).

However, research with indano-3-oxa-2-silacyclopentane derivatives **5** and 4-oxa-3-silacyclohexane derivatives **6** implied a different mechanism. Treatment of **5** with high concentrations of $Bu_3SnH$ furnished the expected indano-3-oxa-2-silacyclopentanes **11**. However, when low tin hydride concentrations were employed a mixture of **11**, together with the ring-enlarged **12**, was obtained.[9] By way of contrast, tin hydride treatment of **6** yielded *only* 4-oxa-3-silacyclohexanes **12**. These results implied that 3-oxa-2-silacyclopentylmethyl radical **7** rearranged to 4-oxa-3-silacyclohexyl radical **8** and that this was irreversible. The rearrangement might involve *β*-scission to Si-centered radical **9** followed by readdition in 6-*endo* mode (route i). An alternative possibility was a 1,2-migration of the Si-group via a transition state (TS) such as **10** (route ii).

**Received:** April 27, 2017
**Published:** June 5, 2017

ACS Publications © 2017 American Chemical Society



DOI: 10.1021/acs.joc.7b01011
J. Org. Chem. 2017, 82, 6886−6894

Deuterium substitution experiments confirmed the basic details of the ring enlargement.[1,9]

Literature precedents favored the elimination route (i). First, because 6-*endo*-ring closure of Si-centered radicals was known to be preferred over the 5-*exo*-mode.[10−13] Then second, route (ii) is a particular example of a 1,2-silicon shift from carbon to carbon. 1,2-Silicon shifts from carbon to carbon were unknown in solution,[14] although 1,2-silicon shifts from carbon to nitrogen[15,16] and from carbon to oxygen[16,17] were well established. Ab-initio QM computations predicted carbon to carbon 1,2-silicon shifts to have high activation barriers (23−25 kcal $mol^{-1}$)[18] so the 1,2-migration route (ii) appeared improbable.

Contrary to expectation, evidence favoring 1,2-migration route (ii) was soon obtained. Radical mediated reactions with chiral phenylselanyl precursors **5c,d** revealed that the configuration at the Si-atoms was *retained* during their ring enlargements. This was inconsistent with route (i) participation by Si-centered radical **9**. In addition, analogous experiments with a deuterium-labeled precursor, 1-vinylsiloxy-4,4-deuterio-4-phenylselano-but-2-ene (**13**, Scheme 3) gave no evidence for participation of a ring-opened Si-centered radical;[9] as would be required during a route (i) process. To shed further light on this counterintuitive ring enlargement we undertook EPR spectroscopic and computational studies with several indano-3-oxa-2-silacyclopentane precursors. Our evidence indicated the "forbidden" 1,2-Si-group migration from carbon to carbon did become allowed provided the Si-groups were suitably "tethered". Limits were established for the scope of related "tethered" 1,2-group migrations. The possibility of Si-hyperconjugative stabilization in intermediate 3-oxa-2-silacyclopentylmethyl radicals containing $\beta$-Si-atoms antiperiplanar with respect to the radical centers was checked out by EPR spectroscopy.

**Scheme 2. Ring Enlargement of Indano-3-oxa-2-silacyclopentanes**

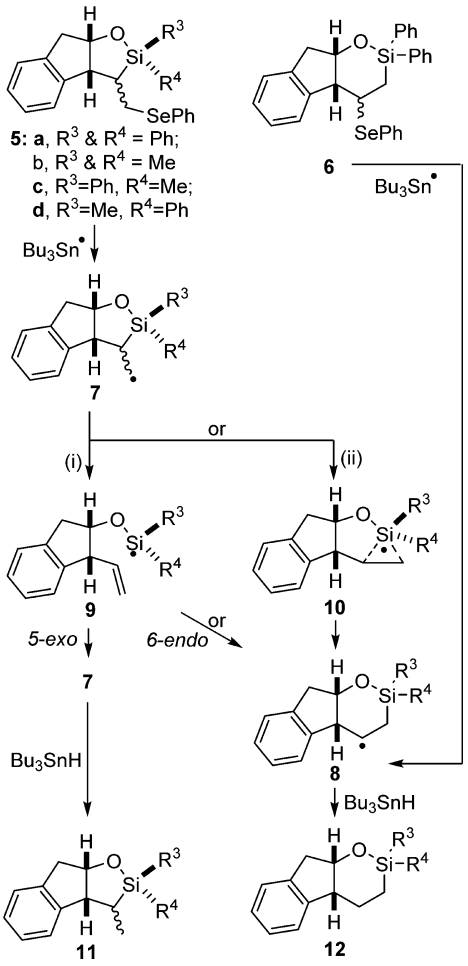


**Scheme 3. Deuterioselano Precursor (13) and Bromomethyl-indano-3-oxa-2-silacyclopentane**

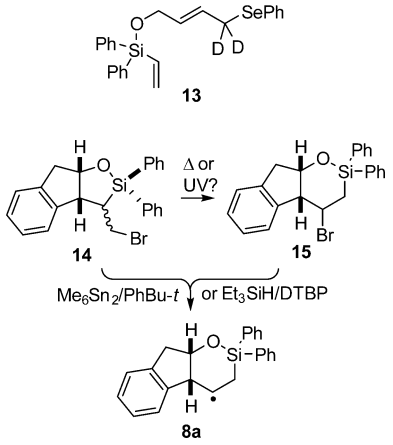


## RESULTS AND DISCUSSION

**EPR Spectroscopic Study of Radical Intermediates.** Organo-bromides are usually excellent precursors for EPR spectroscopic study of transient organic intermediates.[19] We therefore initially planned to use bromomethyl compound **14** (and related molecules) as radical precursors for EPR study of the ring enlargement process. Bromide **14** was prepared by the treatment of **5a** with pyridinium tribromide. When solutions containing **14** and hexamethylditin in PhBu-*t* were UV irradiated, in the resonant cavity of a 9 GHz EPR spectrometer, in the T range 230 to 295 K, transient spectra, obscured by large broad central features, were obtained. After digital filtering a weak signal with the EPR parameters shown in Table 1 was obtained (see Figure S1 in the Supporting Information). Inferior quality spectra resulted when $Et_3SiH$/di-*tert*-butyl peroxide (DTBP) was used in place of ditin as the initiating system. We identify the radical responsible for this spectrum as the rearranged 4-oxa-3-silacyclohexyl radical **8a**. DFT computed hyperfine splittings (hfs) were in reasonable agreement (see Table 1).[20] Careful comparisons with the spectrum of unrearranged radical **7a** (see below) were made but none of this was detectable at any temperature up to 295 K.

The poor signal-to-noise (s/n) of the spectra and the major contribution from broad central features pointed toward degradation of compound **14** on storage and/or during UV irradiation. In view of the fact that only rearranged radical **8a** could be observed, it is possible that precursor **14** had partly rearranged to the 6-member bromo-analogue **15** (Scheme 3). Because of the poor performance of **14** we turned instead to more stable phenylselanyl analogues. The 2,2-diphenyl-compound **5a** and 2,2-dimethyl-compound **5b** (Scheme 2) were prepared by treatment of (±)-1-phenylseleno-2-indanol with the appropriate vinylchlorosilane followed by UV irradiation with hexabutylditin as described previously.[9]



DOI: 10.1021/acs.joc.7b01011
J. Org. Chem. 2017, 82, 6886−6894

**Table 1. Isotropic EPR Parameters of Radicals Generated from Cyclic Alkoxysilanes**[a]

| radical | T/K or QM | g-factor | $a(H^{\alpha})$ | $a(H^{\beta})$ | $a(H^{\gamma})$ | $a(H^{other})$ |
|---|---|---|---|---|---|---|
| **8a** | 260 | 2.0024 | 20.5 (1H) | 7.5 (2H) | | 25.8 (1H) |
| **8a** | DFT(i) | | −23.5 | 3.5, 5.0 | | 21.1 |
| **8a** | DFT(ii) | | −20.8 | 6.2, 22.7 | 1.1 (1H) | 23.0 |
| **8b** | DFT(ii) | | −19.0 | 5.2, 24.4 | 1.2 (1H) | 23.6 ($1H^{\beta}$) |
| **7a** | 260 | 2.0024 | 20.6 (2H) | 18.6 (1H) | <1.0 (1H) | |
| **7a** | DFT(ii) | | −25.8 | 3.6 | −0.8 | |
| **7b(maj)** | 240 | 2.0023 | 20.6 (2H) | 21.3 (1H) | | |
| **7b(x)** | DFT(iii) | | −21.5 | ⟨13.1⟩[b] | −1.5 (1H) | 1.6 ($H^{\delta}$) |
| **7b(min)** | 240 | 2.0023 | 20.6 (2H) | 15.3 (1H) | | |
| **7b(n)** | DFT(iii) | | −19.9 (2H) | ⟨9.1⟩[b] | −0.5 (1H) | 0.02 ($H^{\delta}$) |

[a]Hyperfine splittings (hfs) in Gauss. DFT(i): um062*x*/6-31G(d,p); DFT(ii): UB3LYP/aug-cc-pvtz//UB3LYP/6-31+G(d,p); DFT(iii): UB3LYP/6-311+G(2d,p). [b]Values averaged and weighted by Boltzmann method; see text.

When a solution of **5a** and $Me_6Sn_2$ in PhBu-*t* was UV irradiated in the resonant cavity of the EPR spectrometer a clear triplet of doublets spectrum was obtained in the temperature range 220 to 260 K (EPR parameters in Table 1). This was readily recognized as the unrearranged 3-oxa-2-silacyclopentylmethyl radical **7a** and this identification was supported by DFT computations of the hfs (Table 1). Evidently the $Me_3Sn^{\bullet}$ radical, formed by photodissociation of the hexamethylditin, selectively attacked **5a** at Se and displaced the PhSe group, with production of radical **7a**. At 270 K a new spectrum started to appear and increased in intensity as temperature was raised; see Figure 1 (a) for the 290 K

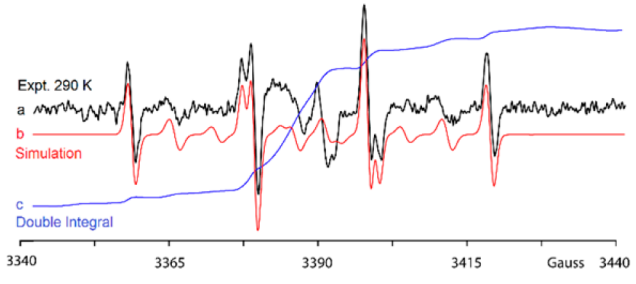


**Figure 1.** (a, black) 9 GHz EPR spectrum during UV irradiation of **5a** and $Me_6Sn_2$ in PhBu-*t* at 290 K; (b, red) computer simulation including both radicals **7a** and **8a**; (c, blue) double integral of the experimental spectrum.

spectrum. The EPR parameters of the new spectrum were essentially identical to those of the rearranged radical **8a** (Table 1). We concluded that the ring enlargement became competitive at $T > 260$ K.

Transient Si-centered radicals of general type **9** are readily detectable by EPR in solution and their spectra are well-known.[21] A DFT optimized structure of radical **9a** [B3LYP/6-31+G(d,p)] had the following EPR hfs: $a(^{29}Si) = -161.4$, $a(2H^{o}) = -0.8$, $a(2H^{m}) = 0.8$, $a(H^{p}) = -1.2$, $a(2H^{o}) = -0.1$, $a(2H^{m}) = 0.6$, $a(H^{p}) = -0.6$ G. However, no EPR signals attributable to this ring-opened radical were detected at any temperature.

Solutions of 2,2-dimethylindano-3-oxa-2-silacyclopentane **5b** and $Me_6Sn_2$ in PhBu-*t*[22] were also irradiated in the EPR cavity. The spectra in the T range 220−310 K showed the presence of two transient radicals both having triplet of doublets splitting patterns (see Figure 2).[23] The EPR parameters indicated these

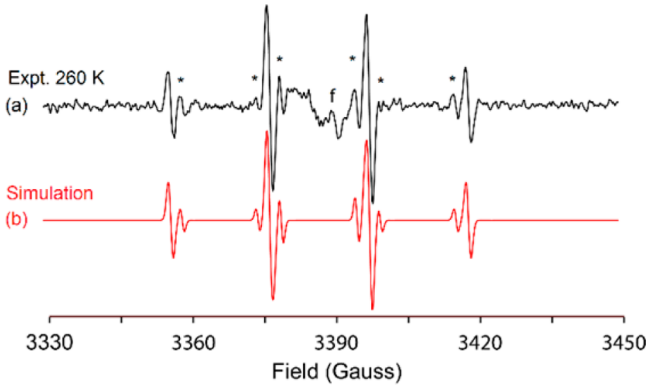


**Figure 2.** Nine GHz EPR spectrum during UV irradiation of **5b** and $Me_6Sn_2$ in PhBu-*t* at 260 K. *Indicates the spectrum of the minor isomer **7b**(min). The feature marked "f" is a background signal from the quartz tube.

species were two isomeric 3-oxa-2-silacyclopentylmethyl radicals **7b(maj,min)** and DFT computations supported this identification (see Table 1). The ratio major:minor was close to 4:1 throughout the whole temperature range. This mirrored the (NMR) ratio of major and minor isomers of the phenylselanyl precursors **5b**; implying that SePh displacement is equally efficient from both isomers. No spectra from the rearranged radical **8b** could be detected even at 310 K hence the ring enlargement takes place more slowly for the 2,2-dimethyl-substituted **7b** than for the 2,2-diphenyl analogue. A DFT optimized structure of ring-opened Si-centered radical **9b** [B3LYP/aug-cc-cptz)//B3LYP/6-31+G(d,p)] had the following EPR hfs: $a(^{29}Si) = -183.0$, $a(6H) = 4.4$ G. No EPR signals attributable to **9b** were detected at any temperature either.

A good deal of information about the structures and conformations of the transient radicals can be gleaned from their EPR data. The hfs of the $H^{\alpha}$-atoms of all the radicals **7a**, **7b** and **8a** are close to 22 G so the radical centers are essentially planar.[20,24] The main difference between the spectra of the two dimethyl **7b** radicals was that the minor isomer had a smaller hfs from its $H^{\beta}$-atom. These $a(H^{\beta})$ hfs of both radicals **7a** and **7b** were smaller than 26.9 G/independent of *T*, which is the norm indicating free rotation about $C^{\beta}-C^{\alpha}$ bonds. Internal rotation about the $^{\bullet}C^{\alpha}H_2-C^{\beta}H$ bonds of radicals **7a** and **7b(maj,min)** was therefore somewhat hindered. The $a(H^{\beta})$ of the diphenyl **7a** and minor dimethyl **7b** increased with temperature as shown on Figure 3. The $a(H^{\beta})$ from the major **7b** isomer was not resolved from $a(H^{\alpha})$ so only rough estimates from computer simulations of the spectra at each temperature are depicted in Figure 3.

These trends implied that their ground state (GS) conformations are as represented in Newman projection **7t** (Chart 1) with their $C^{\beta}-H^{\beta}$ bonds in the nodal plane of their SOMOs. Hence their dihedral angles $\theta°$ between the SOMO axis and the $C^{\beta}-H^{\beta}$ bonds will be about 90°. Silicon substituents $\beta$- to *cationic* centers are known to cause significant


DOI: 10.1021/acs.joc.7b01011
J. Org. Chem. 2017, 82, 6886−6894

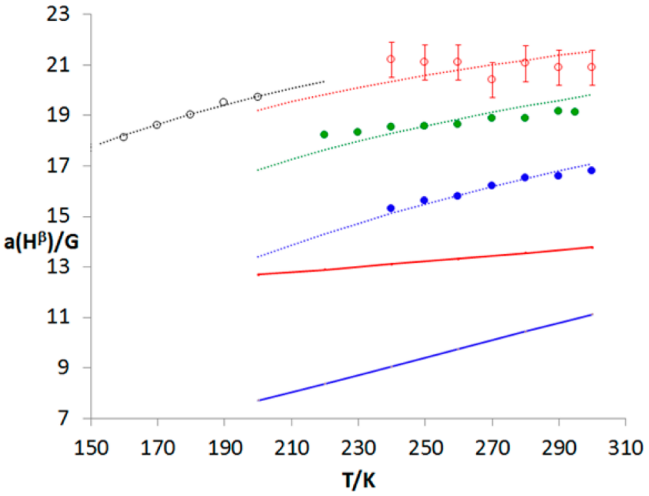


**Figure 3.** Experimental and theoretical temperature dependence of $a(H^{\beta})$ from radicals **7a,b**. Green circles: diphenyl-radical **7a**; blue circles: dimethyl-radical **7b(min)**; red circles: dimethyl-radical **7b(maj)**; black circles: archetype cyclopentylmethyl radical **16**. The dotted lines are values calculated from CL theory. Full lines are from DFT computations (see text).

**Chart 1. Stereochemistry of 3-Oxa-2-silacyclopentylmethyl and Related Radicals**

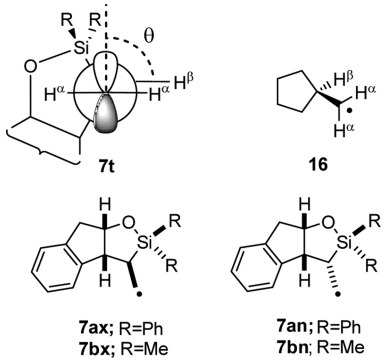


stabilization (Si hyperconjugation); provided there is an antiperiplanar relationship between the empty p-orbital of the carbocation and the filled $\sigma$-molecular orbital of the Si–C bond.[25−28] All three radicals **7a**, **7b(maj,min)** contain the unit $HC(SiR_3)CH_2^{\bullet}$ having Si-atoms $\beta$-to the radical center. Structure **7t** illustrates that the preferred conformations of these radicals have their semioccupied p-orbitals close to antiperiplanar with respect to their Si–C bonds. Does this imply that Si hyperconjugation also stabilizes adjacent radical centers? If this were the case, some double bond character would be associated with the $^{\bullet}C^{\alpha}H_2-C^{\beta}H$ bonds, leading to appreciable barriers to internal rotation.

Rotations (torsions) about the $^{\bullet}C^{\alpha}H_2-C_{\beta}H$ bonds of radicals like **7a,b** are usually controlled by 2-fold sinusoidal potential functions (see below). The magnitudes of the energy barriers ($V_T$) to this torsional motion can be determined from the temperature dependence of the $a(H^{\beta})$ by means of the "Classical Limit" (CL) theory.[29,30] For a given $V_T$ value the theory generates $a(H^{\beta})$ values as a function of temperature and these are compared with the EPR experimental $a(H^{\beta})$ temperature variation. The $V_T$ value can then be derived from the best fit between theory and experiment.[31] The experimental $a(H^{\beta})$ data for radicals **7a** and **7b** is compared in Figure 3 with values derived from CL theory (dotted lines).

Except for radical **7b(maj)**, for which the EPR data was very uncertain, good correspondence with experiment was achieved and the resulting $V_T$ values are listed in Table 2. Comparison with the data of the archetype cyclopentylmethyl radical **16** (Figure 3 and Table 2) shows the results are very reasonable.

**Table 2. Classical Limit ($V_T$) and Computed ($\Delta E_T$) $C^{\alpha}H_2-C^{\beta}H$ Torsion Barriers for Indano-3-oxa-2-silacyclopentylmethyl (7) and Related Radicals[a]**

| radical | method | $V_T$[a] | $\Delta E_T$[a] |
|---|---|---|---|
| **16** | EPR/CL[b] | 1.75 | |
| **16** | DFT(i) | | 0.59 |
| **7a** | EPR/CL[b] | 2.60 | |
| **7a** | DFT(ii) | | 3.39 |
| **7b(maj)** | EPR/CL[b] | 1.90 | |
| **7bx(1)** | DFT(i) | | 3.68 |
| **7bx(2)** | DFT(i) | | 2.86 |
| **7b(min)** | EPR/CL[b] | 3.80 | |
| **7bn(1)** | DFT(i) | | 2.67 |
| **7bn(2)** | DFT(i) | | 2.30 |

[a]Torsion barriers in kcal $mol^{-1}$. [b]CL fit to EPR data. DFT(i): UB3LYP/6-311+G(2d,p). DFT(ii): UB3LYP/6-31G(d,p).

The torsion barrier ($V_T$) found for the minor isomer **7b(min)** was greater than that for the major isomer **7b(maj)**. It follows that radical **7b(min)** was very probably the *endo*-radical **7bn** (Chart 1) because steric hindrance to the $^{\bullet}C^{\alpha}H_2-C^{\beta}H$ torsion will be greater, leading to a higher barrier, in this isomer. Similarly, radical **7b(maj)** can be identified as the *exo*-enantiomer **7bx**.

The measured rotation barriers for **7a** and **7b(maj,min)** are all comparatively small and differ from that of cyclopentylmethyl by ≤2 kcal $mol^{-1}$. It is safe to conclude, therefore, that Si-hyperconjugation in these radicals is insignificant and that any stabilization would be trivial.

To shed further light on the conformational characteristics of the system, DFT computations were carried out for dimethyl-radicals **7bx** and **7bn**. Previous research with cycloalkylmethyl type radicals indicated that the 6-311+G(2d,p) basis set gave results as good as much more extensive triple-$\zeta$ basis sets;[32] so this method was adopted here. Interestingly, *two* minimum energy structures were obtained for the *exo*-isomer **7bx** and these are illustrated in Figure 4.[33]

The main difference between the two *exo* structures was that in **7bx**(1) the pucker at the Si-atom in the 5-member ring

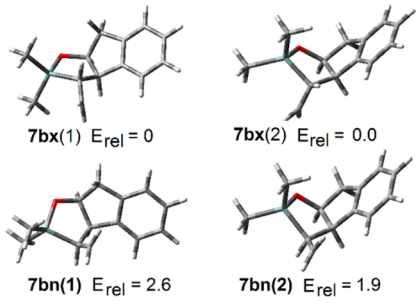


**Figure 4.** DFT computed structures and relative energies (kcal $mol^{-1}$) for *exo*- and *endo*-isomers of radicals **7b**.



DOI: 10.1021/acs.joc.7b01011
J. Org. Chem. 2017, 82, 6886−6894

pointed away from the Indane moiety whereas in **7bx**(2) it pointed toward the Indane moiety. Structures **7bx**(1) and **7bx**(2) had essentially the same energies so, in solution under EPR conditions, both would be populated. At the same level of theory two minimum energy structures were also obtained for the *endo*-isomer **7bn**, again differing in the direction of the pucker in the 5-member oxasilole ring. The energy difference was only 0.63 kcal mol$^{-1}$ so both were probably populated. Note that the structures all had essentially planar radical centers. Furthermore, their predicted conformations about the $^{\bullet}C^{\alpha}H_2-C^{\beta}H$ bond were very similar to that shown in structure **7t** (Chart 1), in good agreement with the EPR experimental observations.

We made DFT examinations of internal rotations about the $^{\bullet}C^{\alpha}H_2-C^{\beta}H$ bonds of each of these isomers. 2-fold rotational potentials were obtained for **7bx**(1), **7bx**(2) and **7bn**(1) with nearly sinusoidal forms. The potential function for **7bn**(2) was similar but with an additional shoulder (see Figure S4 in the Supporting Information). The small asymmetries were expected because of the structural asymmetry in each radical. The rotation barriers ($\Delta E_T$) obtained from these computed potential functions are listed in Table 2 for comparison with the EPR derived barriers.

The $a(H^{\beta})$ hfs were computed at 10° intervals of the dihedral angles $\theta$ for the **7bx**(1) and **7bn**(1) torsions. DFT estimates of the temperature dependencies of $a(H^{\beta})$ for the two radicals were then obtained by Boltzmann averaging as described previously.[32] The average $\langle a(H^{\beta})\rangle$ for **7bx** and **7bn** at particular temperatures are included in Table 1 and the full lines in Figure 3 illustrate the temperature variation computed in this way. These computed hfs significantly underestimate the experimental $a(H^{\beta})$ of **7bx** and **7bn**. Note that such EPR parameters represent an extreme test of the DFT method; it is pleasing that the trend in $a(H^{\beta})$ is reproduced for both **7bx** and **7bn** and the magnitudes are in the right ball park. Similarly, the computed torsion barriers ($\Delta E_T$ in Table 2) were of comparable magnitude to the experimental EPR/CL barriers ($V_T$) but did not reproduce the order for **7bx** and **7bn**.

**Kinetics of the Ring Enlargement Rearrangement.** Assuming the steady state approximation, the rate equation for the 1,2-silyl group migration will be given by eq 1:[34]

$$k_r/2k_t = [\mathbf{8a}] + [\mathbf{8a}]^2/[\mathbf{7a}] \quad (1)$$

where $k_r$ is the rearrangement rate constant and $2k_t$ is the rate constant for radical terminations. Radicals **7a** and **8a** are transient C-centered species so their terminations will be at the diffusion controlled limit. The accurate parameters for C-centered *t*-Bu$^{\bullet}$ radicals [log $A_t$ = 11.63 M$^{-1}$ s$^{-1}$, $E_t$ = 2.25 kcal mol$^{-1}$] determined by Fischer and co-workers,[35] suitably corrected for the viscosity of solvent PhBu-*t* as described previously[36] were, therefore, the best choice for $2k_t$.

As mentioned above, EPR spectra for the diphenyl-indano-3-oxa-2-silacyclopentylmethyl radical **7a** together with its ring-expanded counterpart **8a** were observed by EPR spectroscopy at $T$ > 270 K (see Figure 1). The concentrations [**7a**] and [**8a**] were determined from EPR spectra in the $T$ range 271−307 K. The data was analyzed in two ways: first by double integration of suitable signals from each radical. Second from the double integrals of fully resolved peaks for radical **8a**, combined with the [**7a**]/[**8a**] ratio obtained from computer simulations of the spectra. Individual concentrations and the corresponding $k_r$ values, as well as the Arrhenius plot (Figure S2) are in the Supporting Information. The graph demonstrated the good consistency obtained between the two methods. The accessible temperature range was too short for a reliable Arrhenius A-factor to be derived from the data. However, first order reactions of this type normally[14a] have Log($A/s^{-1}$) factors of ca. 11.0 and, assuming this holds, the resulting rate parameters are

$$E_r = 12.6 \pm 1.5 \text{ kcal mol}^{-1} \quad k_r(300 \text{ K}) = 64 \text{ s}^{-1}$$

None of the ring-expanded radical **8b** was detectable in EPR spectra from the dimethyl-indano-3-oxa-2-silacyclopentylmethyl radicals **7b** at the highest accessible temperature (310 K) so kinetic EPR could not be undertaken. It was apparent, therefore, that the 1,2-migration was significantly slower when the Si-atom carried Me instead of Ph substituents. However, an estimate of the lower limit of $E_r$ (≥14.5 kcal mol$^{-1}$) was obtained from EPR measurement of [**7b**] and the spectral s/n at 310 K (see Supporting Information). This EPR derived activation energy for **7a** ring expansion was marginally greater than that obtained by the radical clock method.[2]

The rates of radical 1,2-group migrations are usually faster for migrating groups better able to accommodate the unpaired electron (upe) during the transfer.[14] Ph substituents on Si would be expected to better delocalize the upe in a migrating $SiR_2$ group than Me substituents. The slower ring enlargement rearrangement and higher $E_r$ of the dimethyl-radical **7b** make good sense therefore.

Kinetic data for cyclizations of Si-centered radicals is sparse. Available rate constants[13,10] of 6-*endo* ring closures are orders of magnitude greater ($10^7$ to $10^9$ s$^{-1}$) than that obtained for the rearrangement of **7a** (see above and Table 3). Kinetic evidence therefore also militates against the route (i) mechanism involving dissociation followed by 6-*endo*-cyclization of Si-centered radical **9**.

**Table 3. Experimental and Computed Reaction Parameters (kcal mol$^{-1}$) for Radical Ring Enlargement of 1,2-Oxasilolanes**

| radical | R ($SiR_2$) | method | | | $E_r$[a] | |
|---|---|---|---|---|---|---|
| **7a** | $Ph_2$ | EPR | | | 12.6 | |
| **7a** | $Ph_2$ | RadCk[b] | | | 10.6 | |
| **7b** | $Me_2$ | EPR | | | ≥14.5 | |
| **7b** | $Me_2$ | RadCk[b] | | | 12.4 | |
| | | | $\Delta H°$ | $\Delta G°$ | $\Delta H^{‡}$ | $\Delta G^{‡}$ |
| **17a** | $Ph_2$ | DFT(i) | −8.2 | −8.2 | 13.6 | 14.7 |
| **17a** | $Ph_2$ | DFT(ii) | −7.8 | −7.8 | 12.8 | 13.9 |
| **17b** | $Me_2$ | DFT(i) | −7.6 | −6.8 | 14.3 | 15.6 |
| **17b** | $Me_2$ | DFT(ii) | −7.5 | −7.0 | 13.0 | 14.8 |
| **17b** | $Me_2$ | DFT(iii) | −7.8 | −7.0 | 14.0 | 15.3 |
| **17c** | $Me_2$ | DFT(iii) | −7.9 | −7.4 | 14.7 | 15.7 |

[a]Experimental Arrhenius activation energies (kcal mol$^{-1}$). [b]Radical clock method ref 2; DFT(i): UB3LYP/6-31+G(d,p), DFT(ii): UM062*X*/6-31G(d,p), DFT(iii): UB3LYP/aug-cc-pvtz//UB3LYP/6-31+G(d,p).

**QM Computational Study of Oxasilole Ring Expansion.** To obtain theoretical insight into the mechanism of the ring enlargement, molecular structures and reaction enthalpies were computed with the Gaussian 09.D01 suite of programs.[37] Structures were fully optimized and frequency calculations enabled enthalpies and Gibbs free energies to be obtained that included zero point energies and thermal corrections to 298 K.



DOI: 10.1021/acs.joc.7b01011
J. Org. Chem. 2017, 82, 6886−6894

Prototypical 2,2-dimethyl-1,2-oxasilolanylmethyl radicals **17a,b** were chosen to model the system and computations were carried out with the UM062X/6-31G(d,p) method,[38] the UB3LYP/6-31+G(d,p) method and with the UB3LYP/aug-cc-PVTZ//UB3LYP/6-31+G(d,p) method.[39−41] Only the former methods were applied to the computationally much more demanding diphenyl system.

Energies computed by the UB3LYP and UM062X methods were reasonably close (Table 3). In agreement with the experimental outcome for indano-analogues (**7a** and **7b**) the $\Delta H^{\ddagger}$ and $\Delta G^{\ddagger}$ activation barriers for the 1,2-shift of the $SiPh_2$ group were computed to be less than for the $SiMe_2$ group.

Enthalpies of each species, relative to that of the dimethyl-radical **17b**, are illustrated in Figure 5. The 6-member ring

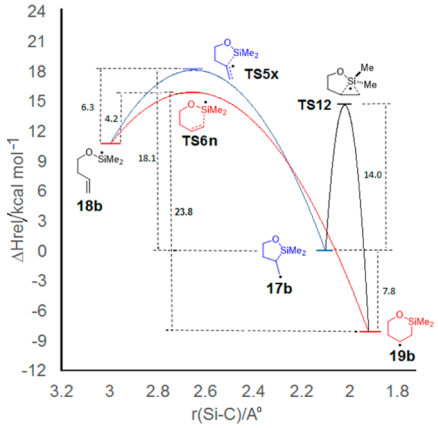


**Figure 5.** Relative DFT enthalpies ($\Delta H°$) and activation enthalpies ($\Delta H^{\ddagger}$/kcal mol$^{-1}$) for ring enlargement of radical **17b** [UB3LYP/aug-cc-PVTZ//UB3LYP/6-31+G(d,p)].

radical **19b** was 7.8 kcal mol$^{-1}$ lower in energy than the 5-member reactant **17b**. The $\Delta H^{\ddagger}$ for the 1,2-migration of the $SiMe_2$ group (14 kcal mol$^{-1}$) was significantly less than $\Delta H^{\ddagger}$ for opening of the 5-member ring (18.1 kcal mol$^{-1}$) and production of Si-centered radical **18b** (or opening of the 6-member ring; 23.8 kcal mol$^{-1}$). Thus, DFT predicted that the 1,2-migration route (ii) would be the prevailing mechanism. This is in accord with the EPR and other experimental data for related indano-radicals **7** (see above). Furthermore, the computed $\Delta H^{\ddagger}$ is within the experimental error limits of the experimental activation energies (Table 3) for ring enlargement of radical **7b**. The $\Delta H^{\ddagger}$ of the reverse 1,2-shift from **19b** to **17b** (21.8 kcal mol$^{-1}$) is sufficiently high to preclude this; also in agreement with experiments from radicals **7a,b**. A further point to notice is the small computed $\Delta H^{\ddagger}$ for 6-*endo*-cyclization of radical **18b** (4.2 kcal mol$^{-1}$). This implies a very rapid process; in agreement with literature kinetic data noted earlier,[10,13]

The calculated [UB3LYP/6-31+G(d,p)][42] geometry and SOMO of the transition state of the 1,2-$SiMe_2$ migration (**TS12**) in radical **17b** are displayed in Figure 6. The TSs for 5-*exo*- and 6-*endo*-ring closures are in the Supporting Information (Figure S3). In **TS5x** and **TS6n** the forming/breaking Si···C bonds are comparatively long (2.65 and 2.72 Å respectively) and the $C^{\alpha}-C^{\beta}$ (acceptor) bond lengths differ little from typical double bonds. In accord with this, the SOMOs have high density associated with the Si-atoms and the $C^{\alpha}-C^{\beta}$ bonds. Both TSs are "late" for ring opening (early for cyclization). The **TS12** has much shorter Si−C bonds and the $C^{\alpha}-C^{\beta}$ bond is considerably longer than a typical double bond. The

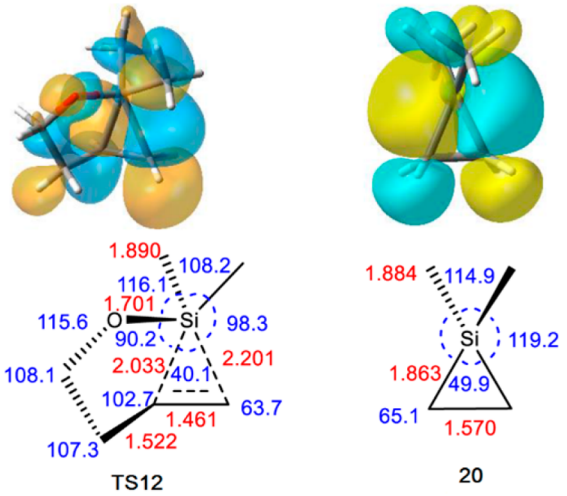


**Figure 6.** DFT computed TS structures and SOMOs.

dimensions of **TS12** are close to those obtained by Schiesser and Styles from their ab initio study of the degenerate 1,2-$SiH_3$ shift in the 2-silylethyl radical [$H_3SiCH_2CH_2^{\bullet} \rightarrow {}^{\bullet}CH_2CH_2SiH_3$].[18] The geometry of **TS12** is similar to that of a silacyclopropane ring slightly stretched at the Si-apex (compare structure **20**). The SOMO of **TS12** displays high density associated with the 3-member $SiC^{\alpha}C^{\beta}$ ring. Furthermore, it too resembles the in plane $\pi$-system of the HOMO of silacyclopropane (see structure **20**, Figure 6).

This "double bond character"[43] may be a factor in lowering the energy of the TS. Schiesser and Styles reported that the groups attached to Si formed a tetrahedral arrangement resembling a "coordinated alkene". During the 1,2-ring enlargement of **17b** the Si group remains "tethered" via oxygen throughout the process, unlike the 2-silylethyl rearrangement. As expected, therefore, the $SiC^{\alpha}C^{\beta}$ triangle in **TS12** is slightly skewed toward the oxygen tether. Otherwise the arrangement of ligands around Si is also closer to an irregular-tetrahedron than to a trigonal bipyramid.

The main difference from the 2-silylethyl migration is in the predicted activation parameters. Schiesser and Styles obtained 23.0−25.2 kcal mol$^{-1}$ (depending on the computational method) for this process. Our computed activation barriers for ring enlargements of **17a,b** were lower by the chemically very significant factor of about 10 kcal mol$^{-1}$. Thus, QM computations capably reproduce what is known experimentally. That is, conventional 1,2-silicon shifts from carbon to carbon do not occur in solution; nevertheless the tethered variety, as found in 5- to 6-member oxasilole ring enlargements, have low enough barriers to proceed.

To assess the role of the ring O atom, the ring enlargement of the 1,1-dimethylsilolanylmethyl radical **17c**, that lacks this O atom, was also investigated by DFT. The structure of **TS12c** for the tethered 1,2 Si-migration was closely similar to that of Figure 6 [r(Si−$C^{\alpha}$) = 2.03, r(Si−$C^{\beta}$) = 2.21 Å, ∠$C^{\alpha}SiC^{\beta}$ = 40.0°]. The energetics of the **17c** rearrangement were also found to be only marginally more exoenthalpic (compare with **17b** in Table 3). Correspondingly, the $\Delta H^{\ddagger}$ and $\Delta G^{\ddagger}$ activation barriers were only 0.7 and 0.4 kcal mol$^{-1}$ greater respectively than their counterparts in the O-containing system (**17b**).



DOI: 10.1021/acs.joc.7b01011
J. Org. Chem. 2017, 82, 6886−6894

## CONCLUSIONS

EPR spectra obtained during irradiations of derivatives of the indano-oxasilacyclopentane systems (**5a,b**) revealed none of the ring-opened Si-centered radicals **9a** or **9b** at any temperature from 220 to 310 K. This was strong evidence opposed to the elimination-readdition mechanism [route (i)] for the ring enlargement. DFT computations with model 2,2-dimethyl-1,2-oxasilolanylmethyl radicals (**17a,b**) also predicted the 1,2-migration ring enlargement pathway [route (ii)] to be lower in energy than the route (i) pathway. The computed structures around Si in the TSs of the "tethered" 1,2-Si group migrations were all quasi-tetrahedral, resembling coordinated alkenes.

The EPR spectra of oxasilolano-methyl radicals (**7a,b**) disclosed that in their preferred GS conformations their semioccupied p-orbitals were positioned close to *antiperiplanar* with respect to their $\beta$-Si−C bonds. We found experimentally and computationally that in our radical species the torsion barriers around the $^{\bullet}C^{\alpha}H_2-C^{\beta}Si(H)$ bonds were of the same magnitude as for typical $^{\bullet}C^{\alpha}H_2-C^{\beta}C(H)$ bonds. Consequently, hyperconjugative stabilization by $\beta$-Si-atoms can probably be discounted for free radicals.

Rate parameters, obtained by steady-state kinetic EPR, for the ring expansion of diphenyl-radical **7a** were in reasonable agreement with previous data from radical clock experiments. Demonstrably, therefore, the activation energy required for the "tethered" 1,2-Si shift in oxasilole ring enlargement was much lower than for a conventional, unconstrained, Si-1,2-shift from carbon to carbon. What explanation can be offered for this? Several factors probably contribute. In the 2-silylethyl migration both initial and final radicals are *primary* whereas the ring enlargements of **7a,b** (and **17a,b**) convert *primary* radicals to *secondary* radicals. The latter are about 2.5 kcal mol$^{-1}$ thermodynamically more stabilized.[44] In the tethered processes the rings enlarge from 5- to 6-member. For oxasilole rings the relief of ring strain entailed will be[45] 3.5−4.5 kcal mol$^{-1}$. A further factor could be that dimensional reorganization (Si−C bond stretching and contracting, angle opening and closing) in forming the compact **TS12** will be minimal. As judged by the energetics for the nonoxygen-containing model **17c**, the O atom in the tether assists the rearrangement by a small factor (~0.5 kcal mol$^{-1}$).

Can analogous ring enlargements via concerted 1,2-Si shifts be expected for other ring systems? The magnitude of the computed activation parameters for the silacyclopentane system **17c** ($\Delta H^{\ddagger}$ = 14.7 kcal mol$^{-1}$) signifies that ring expansion should readily take place in solution for compounds containing this unit. This will extend preparative opportunities for this tactic, which is attractive because of its retention of stereochemistry. Ring expansion of a 6-member oxasilolylmethyl radical [2,2-trimethyl-1,2-oxasilinanylmethyl] to the 7-member species [2,2-dimethyl-1,2-oxasilepanyl radical] will actually entail a small *increase* in ring strain. The consequent increased activation energy would probably push the required temperature above normal solution phase conditions. For the 4-member oxasiloylmethyl radical [2,2-dimethyl-1,2-oxasiletanylmethyl] ring expansion to the 5-member ring would entail large ring strain relief. However, in this case, complete ring opening to the Si-centered allyloxysilanyl radical would be highly exoenthalpic, so straight chain products are likely to dominate. Probably, therefore, ring expansion via tethered 1,2-Si shifts from C to C will be restricted to 5-member ring types. Of course, ring expansions by 1,2-Si-shifts from C to N and C to O can also be expected with cyclic-oxasilolyl-aminyl and -oxasilolyl-oxyl radicals.

1,2-Alkyl group migrations from carbon to carbon are also unknown in solution.[14] The success of the tethered Si-group migration raised the possibility that ring enlargement via tethered alkyl groups might occur via a concerted 1,2-alkyl shifts. Model tetrahydrofuranylmethyl radical **21** (Scheme 4) is the carbon analogue of **17b**. A DFT computation [UB3LYP/6-31G(d,p)] with this indicated the 1,2-ring expansion would be exoenthalpic by ~6 kcal mol$^{-1}$ but that the enthalpy of activation would be prohibitively high at 55 kcal mol$^{-1}$ (see Supporting Information). This agrees with a published DFT study of the ring expansion of cyclopentylmethyl radical to cyclohexyl radical that predicted an activation barrier of similar magnitude.[46] Hence both conventional and tethered alkyl 1,2-group migrations from carbon to carbon remain "forbidden".

**Scheme 4. Ring Enlargement Options for 2,2-Disubstituted-1,2-Oxasilolanylmethyl Radicals 17a,b**

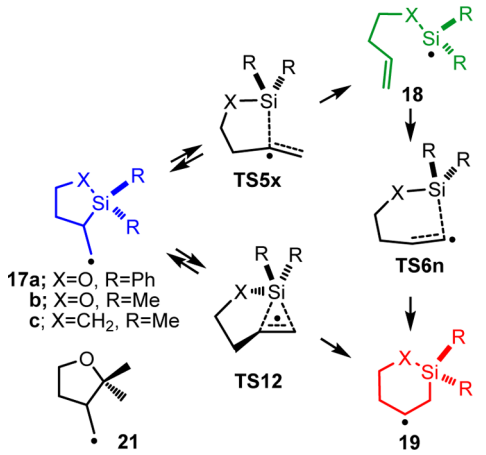


## EXPERIMENTAL DETAILS

Commercially available reagents were used as received. NMR spectra were recorded at 270, 400, or 500 MHz ($^1$H) and at 100 or 125 MHz ($^{13}$C), and are reported in ppm downfield from TMS. Mass spectra were obtained with a T100GCV TOF instrument by electron ionization (EI) or by fast atom bombardment (FAB). Thin layer chromatography was performed on coated plates 60F254. Silica gel chromatography was performed with silica gel 5715. Reactions were carried out under an argon atmosphere. HPLC was performed with SIL-06-s-5 (analytical, 4.6 × 250 mm; preparative, 20 × 250 mm). Compound **5a** and precursors were prepared according to the reported procedures.[9]

**(3aR,8aS)-2,2-Diphenyl-3-bromomethyl-3,3a,8,8a-tetrahydro-2H-indeno[1,2-*d*][1,2]oxasilole (14).** To a solution of compound **5a** (274 mg, 0.55 mmol) in dichloromethane (5.5 mL) was added pyridinium tribromide (177 mg, 0.55 mmol). After the reaction was completed, water was added, and the resulting mixture was partitioned. The organic layer was washed with brine, dried with sodium sulfate, and evaporated. The residue was purified by silica gel column chromatography (EtOAc/hexane) to give Br compound **14** (162 mg, 0.38 mmol): $^1$H NMR (500 MHz, $CDCl_3$) $\delta_H$ 7.62−7.17 (m, 14 H), 5.10−5.06 (m, 1 H), 4.79−4.74 (m, 1 H), 3.64−3.61 (m,1 H), 3.15−3.10 (m, 1 H), 3.03−2.99 (m, 1 H), 2.23−2.19 (m, 1 H), 2.11−2.02 (m, 1 H); $^{13}$C NMR (125 MHz, $CDCl_3$) $\delta_C$ 141.7, 140.7, 134.4, 134.3, 134.2, 134.1, 130.4, 130.3, 128.0, 128.0, 127.1, 126.5, 126.3, 124.9, 77.9, 55.6, 52.5, 40.0, 23.4; LRMS (EI) *m/z* 420, HRMS (EI) calcd for $C_{23}H_{21}BrOSi$: 420.0545 ($M^+$), found 420.0546.

**(±)-*trans*-2-*O*-Dimethylvinylsilyl-1-phenylseleno-2-indanol.** A solution of (1*S*,2*S*)-1-(phenylselanyl)-2,3-dihydro-1*H*-inden-2-ol


DOI: 10.1021/acs.joc.7b01011
J. Org. Chem. 2017, 82, 6886−6894

(1.05 g, 3.63 mmol), $Et_3N$ (0.75 mL, 5.4 mmol), DMAP (44 mg, 0.36 mmol), and dimethylvinylchlorosilane (0.73 mL, 5.40 mmol) in dichloromethane (16 mL) was stirred at room temperature for 5 min. $Et_2O$ and water were added, and the resulting mixture was partitioned. The organic layer was washed with brine, dried ($Na_2SO_4$), and evaporated. The residue was purified by silica gel column chromatography ($Et_2O$/hexane = 1/50) to give the title compound (1.12 g, 83%) as a pale yellow oil: $^1$H NMR (500 MHz, $CDCl_3$) $\delta_H$ 7.56 (d, 2 H, $J$ = 6.6 Hz), 7.34−7.18 (m, 7 H), 6.00−5.92 (m, 2 H), 5.67 (dd, 1 H, $J$ = 20.0, 4.6 Hz), 4.65 (s, 1 H), 4.59 (m, 1 H), 3.25 (dd, 1 H, $J$ = 16.3, 5.4 Hz), 2.77 (d, 1 H, $J$ = 16.3 Hz), 0.07 (s, 3H), 0.05 (s, 3H); $^{13}$C NMR (125 MHz, $CDCl_3$) $\delta_C$ 141.3, 140.9, 137.4, 134.7, 133.2, 129.7, 129.0, 127.8, 127.7, 126.8, 125.6, 125.0, 79.4, 54.7, 40.7, −1.72, −1.80; LRMS (ESI) $m/z$ 397 [(M + Na)+]; HRMS (ESI) calcd for $C_{19}H_{22}NaOSeSi$: 397.0503 [(M + Na)+], found 397.0503; Anal. Calcd for $C_{19}H_{22}OSeSi$: C, 61.11; H, 5.94. Found: C, 60.96; H, 5.71.

**(3a*R*,8a*S*)-2,2-Dimethyl-3-((phenylselanyl)methyl)-3,3a,8,8a-tetrahydro-2*H*-indeno[1,2-*d*][1,2]oxasilole (5b).** A stirred solution of (±)-*trans*-2-*O*-dimethylvinylsilyl-1-phenylseleno-2-indanol (1.00 g, 2.68 mmol) and $(Bu_3Sn)_2$ (270 μL, 540 μmol) in benzene (13.5 mL) was irradiated with a high-pressure mercury lamp (400 W) at room temperature for 7 h. The solvent was evaporated, and the residue was purified by silica gel column chromatography (EtOAc/hexane = 1/35) to give **5b** (436 mg, 44%) as a pale yellow oil: $^1$H NMR (500 MHz, $CDCl_3$) $\delta_H$ 7.59−6.98 (m, 9 H), 4.91 (t, 0.80 H, $J$ = 4.7 Hz), 4.78 (t, 0.20 H, $J$ = 4.9 Hz), 3.83−3.79 (m, 1 H), 3.33−3.29 (m, 1 H), 3.12−3.06 (m, 3 H), 1.94−1.97 (m, 0.2 H), 1.70−1.73 (m, 0.80 H), 0.26 (s, 0.6H), 0.23 (s, 2.4 H), −0.29 (s, 0.6H), −0.36 (s, 2.4 H); $^{13}$C NMR (125 MHz, $CDCl_3$) major isomer $\delta_C$ 144.2, 141.4, 133.5, 132.6, 129.9, 129.2, 127.1, 126.6, 125.1, 124.4, 81.1, 54.8, 41.4, 30.4, 30.3, 0.4, −2.7; LRMS (APCI) $m/z$ 375 [(M + H)+]; HRMS (APCI) calcd for $C_{19}H_{23}OSeSi$: 375.0678 [(M + H)+], found 375.0683.

**Computational Methods.** DFT calculations were carried out using the Gaussian 09 suite of programs.[37] Vibrational frequency calculations were implemented so that TS status could be checked (one imaginary frequency) and enthalpies and free energies were adjusted for zero point and thermal corrections to 1 atm and 298 K. Experimental data referred to neutral radicals in a nonpolar hydrocarbon environment so solvent effects will be insignificant. DFT computations in the gas phase only were therefore carried out.

**CW EPR Spectroscopy.** Isotropic EPR spectra were obtained at 9.5 GHz with 100 kHz modulation employing a commercial spectrometer fitted with a rectangular ER4122 SP resonant cavity. Stock suspensions of each cyclic oxasilyl ether (10 to 20 mg) and $Me_2SnSnMe_2$ (10 to 20 mg) or $Et_3SiH$ (0.02 mL) and di-*t*-butyl peroxide (DTBP, 0.01 mL) in benzene (0.5 mL) or *tert*-butylbenzene (0.5 mL) were prepared and sonicated if necessary. An aliquot (0.25 mL), to which any additional reactant had been added, was placed in a 4 mm o. d. quartz tube, deaerated by bubbling nitrogen for 15 min. Photolysis was in the resonant cavity by unfiltered light from a 500 W super pressure mercury arc lamp. In all cases where spectra were obtained, hfs were assigned with the aid of computer simulations using the SimFonia and NIEHS Winsim2002 software packages. EPR signals were digitally filtered and double integrated using the WinEPR software and radical concentrations were calculated by reference to the double integral of the signal from a known concentration of the stable radical DPPH [$1 \times 10^{-3}$ M in PhMe], run under identical conditions. The majority of EPR spectra were recorded with 2.0−4.0 mW power, 1.0 $G_{pp}$ modulation intensity and gain of ca. $10^6$.

## ■ ASSOCIATED CONTENT

### Supporting Information

The Supporting Information is available free of charge on the ACS Publications website at DOI: 10.1021/acs.joc.7b01011.

EPR and kinetic data, Cartesian coordinates for computed structures, NMR spectra precursors (PDF)

## ■ AUTHOR INFORMATION


### Corresponding Authors

*jcw@st-andrews.ac.uk

*h-abe@chem.nagoya-u.ac.jp

### ORCID

John C. Walton: 0000-0003-2746-6276

Takeaki Iwamoto: 0000-0002-8556-5785

Satoshi Shuto: 0000-0001-7850-8064


### Notes

The authors declare no competing financial interest.

## ■ ACKNOWLEDGMENTS

JCW thanks EaStCHEM for financial support.

## ■ REFERENCES


(1) (a) Shuto, S.; Kanazaki, M.; Ichikawa, S.; Matsuda, A. *J. Org. Chem.* **1997**, *62*, 5676−5677. (b) Sakaguchi, N.; Hirano, S.; Matsuda, A.; Shuto, S. *Org. Lett.* **2006**, *8*, 3291−3294. (c) Mikhaylov, A. A.; Zard, S. Z. *Org. Lett.* **2017**, *19*, 1866−1869.

(2) Sugimoto, I.; Shuto, S.; Matsuda, A. *Synlett* **1999**, *1999*, 1766−1768.

(3) Tamao, K.; Ishida, N.; Kumada, M. *J. Org. Chem.* **1983**, *48*, 2122−2124.

(4) Jones, G. R.; Landais, Y. *Tetrahedron* **1996**, *52*, 7599−7662.

(5) (a) Shuto, S.; Kanazaki, M.; Ichikawa, S.; Minakawa, N.; Matsuda, A. *J. Org. Chem.* **1998**, *63*, 746−754. (b) Sato, T.; Tsuzuki, T.; Takano, S.; Kato, K.; Fukuda, H.; Arisawa, M.; Shuto, S. *Tetrahedron* **2015**, *71*, 5407−5413.

(6) Shuto, S.; Yahiro, Y.; Ichikawa, S.; Matsuda, A. *J. Org. Chem.* **2000**, *65*, 5547−5557.

(7) Terauchi, M.; Yahiro, Y.; Abe, H.; Ichikawa, S.; Tovey, S. C.; Dedos, S. G.; Taylor, C. W.; Potter, B. V. L; Matsuda, A.; Shuto, S. *Tetrahedron* **2005**, *61* (61), 3697−3707.

(8) (a) Ueno, Y.; Nagasawa, Y.; Sugimoto, I.; Kojima, N.; Kanazaki, M.; Shuto, S.; Matsuda, A. *J. Org. Chem.* **1998**, *63*, 1660−1667. (b) Sugimoto, I.; Shuto, S.; Mori, S.; Shigeta, S.; Matsuda, A. *Bioorg. Med. Chem. Lett.* **1999**, *9*, 385−388.

(9) Shuto, S.; Sugimoto, I.; Abe, H.; Matsuda, A. *J. Am. Chem. Soc.* **2000**, *122*, 1343−1351.

(10) Chatgilialoglu, C.; Woynar, H.; Ingold, K. U.; Davies, A. G. *J. Chem. Soc., Perkin Trans. 2* **1983**, 555−565.

(11) Barton, T. J.; Revis, A. *J. Am. Chem. Soc.* **1984**, *106*, 3802−3805.

(12) Sarasa, J. P.; Igual, J.; Poblet, J. M. *J. Chem. Soc., Perkin Trans. 2* **1986**, 861−865.

(13) For a review, see: Chatgilialoglu, C. In *Organosilanes in Radical Chemistry*; Wiley: Chichester, 2004; pp 119−142.

(14) For reviews, see: (a) Beckwith, A. L. J.; Ingold, K. U. In *Rearrangements in Ground and Excited States*; De Mayo, P., Ed.; Elsevier: New York, 1980; Vol. *1*, pp 162−310. (b) Chatgilialoglu, C. In *Organosilanes in Radical Chemistry*; Wiley: Chichester, 2004; pp 137−142.

(15) West, R.; Boudjouk, P. *J. Am. Chem. Soc.* **1973**, *95*, 3938−3987.

(16) (a) Harris, J. M.; MacInnes, I.; Walton, J. C.; Maillard, B. *J. Organomet. Chem.* **1991**, *403*, C25−28. (b) Harris, J. M.; Walton, J. C.; Maillard, B.; Grelier, S.; Picard, J.-P. *J. Chem. Soc., Perkin Trans. 2* **1993**, 2119−2123.

(17) Roberts, B. P.; Vazquez-Persaud, A. R. *J. Chem. Soc., Perkin Trans. 2* **1995**, 1087−1095.

(18) Schiesser, C. H.; Styles, M. L. *J. Chem. Soc., Perkin Trans. 2* **1997**, 2335−2340.

(19) Walton, J. C. In *Encyclopedia of Radicals in Chemistry, Biology and Materials*; Chatgilialoglu, C., Studer, A., Eds.; Wiley: Chichester, U.K., 2012; Vol. *1*, Chapter 7, pp 147−174.

(20) The computed structure of the 6-member 4-oxa-3-silacyclohexyl ring of **8a** is a quasi-chair. It is probable this undergoes rapid inversion in solution such that the $H^{\beta}$-atoms of the $CH_2$ group adjacent to the




DOI: 10.1021/acs.joc.7b01011
*J. Org. Chem.* 2017, 82, 6886−6894

radical center appear equivalent on the EPR time scale and hence produce the triplet hfs (7.5 G, Table 1). This should be compared with the average of the DFT computed $a(H^{\beta})$ in Table 1.
(21) Chatgilialoglu, C. *Chem. Rev.* **1995**, *95*, 1229−1251.
(22) DTBP (ca. 10 mg) as photsensitizer was found to improve the quality of the spectra.
(23) Note that only 4 lines show in the spectrum of the major isomer in Figure 2 because the hfs from the $2H^{\alpha}$ of radical **7b** is not resolved from the hfs of $H^{\beta}$.
(24) Kochi, J. K. *Adv. Free Radical Chem.* **1975**, *5*, 189−317.
(25) Cooper, B. E.; Owen, W. J. *J. Organomet. Chem.* **1971**, *29*, 33−40.
(26) Hase, H. L.; Schweig, A. *Tetrahedron* **1973**, *29*, 1759−1764.
(27) Fleming, I.; Hrovat, D. A.; Borden, W. T. *J. Chem. Soc. Perkin Trans. 2* **2001**, 331−338.
(28) Hassall, K.; Lobachevsky, S.; Schiesser, C. H.; White, J. M. *Organometallics* **2007**, *26*, 1361−1364.
(29) Krusic, P. J.; Kochi, J. K. *J. Am. Chem. Soc.* **1971**, *93*, 846−860.
(30) Kemball, M. L.; Walton, J. C.; Ingold, K. U. *J. Chem. Soc., Perkin Trans. 2* **1982**, 1017−1023.
(31) The potential barriers in radicals **7a**,**b** will not be exactly symmetrical 2-fold sinusoidal as required by classical limit theory. However DFT computations (see below and SI) indicated that errors introduced from this source were not serious.
(32) McBurney, R. T.; Harper, A. D.; Slawin, A. M. Z.; Walton, J. C. *Chem. Sci.* **2012**, *3*, 3436−3444.
(33) Two optimized structures very similar to those in Figure 4 were obtained with the UM062X/6-311+G(2d,p) method but only the UB3LYP/6-311+G(2d,p) data is given here because this method gave better agreement with the experimental EPR data.
(34) (a) Griller, D.; Ingold, K. U. *Acc. Chem. Res.* **1980**, *13*, 200−206. (b) Griller, D.; Ingold, K. U. *Acc. Chem. Res.* **1980**, *13*, 317−323.
(35) (a) Schuh, H.-H.; Fischer, H. *Helv. Chim. Acta* **1978**, *61*, 2130−2164. (b) Schuh, H.-H.; Fischer, H. *Int. J. Chem. Kinet.* **1976**, *8*, 341−356.
(36) (a) Maillard, B.; Walton, J. C. *J. Chem. Soc., Perkin Trans. 2* **1985**, 443−450. (b) Bella, A. F.; Jackson, L. V.; Walton, J. C. *J. Chem. Soc., Perkin Trans. 2* **2002**, 1839−1843.
(37) Frisch, M. J.; Trucks, G. W.; Schlegel, H. B.; Scuseria, G. E.; Robb, M. A.; Cheeseman, J. R.; Scalmani, G.; Barone, V.; Mennucci, B.; Petersson, G. A.; Nakatsuji, H.; Caricato, M.; Li, X.; Hratchian, H. P.; Izmaylov, A. F.; Bloino, J.; Zheng, G.; Sonnenberg, J. L.; Hada, M.; Ehara, M.; Toyota, K.; Fukuda, R.; Hasegawa, J.; Ishida, M.; Nakajima, T.; Honda, Y.; Kitao, O.; Nakai, H.; Vreven, T.; Montgomery, J. A., Jr.; Peralta, J. E.; Ogliaro, F.; Bearpark, M.; Heyd, J. J.; Brothers, E.; Kudin, K. N.; Staroverov, V. N.; Kobayashi, R.; Normand, J.; Raghavachari, K.; Rendell, A.; Burant, J. C.; Iyengar, S. S.; Tomasi, J.; Cossi, M.; Rega, N.; Millam, J. M.; Klene, M.; Knox, J. E.; Cross, J. B.; Bakken, V.; Adamo, C.; Jaramillo, J.; Gomperts, R.; Stratmann, R. E.; Yazyev, O.; Austin, A. J.; Cammi, R.; Pomelli, C.; Ochterski, J. W.; Martin, R. L.; Morokuma, K.; Zakrzewski, V. G.; Voth, G. A.; Salvador, P.; Dannenberg, J. J.; Dapprich, S.; Daniels, A. D.; Farkas, Ö.; Foresman, J. B.; Ortiz, J. V.; Cioslowski, J.; Fox, D. J. *Gaussian 09*, Revision D.01; Gaussian, Inc.: Wallingford, CT, 2013.
(38) Zhao, Y.; Truhlar, D. G. *Theor. Chem. Acc.* **2008**, *120*, 215−241.
(39) Becke, A. D. *J. Chem. Phys.* **1993**, *98*, 5648−5652.
(40) Dunning, T. H., Jr. *J. Chem. Phys.* **1989**, *90*, 1007−1023.
(41) Wilson, A. K.; van Mourik, T.; Dunning, T. H., Jr. *J. Mol. Struct.: THEOCHEM* **1996**, *388*, 339−349.
(42) TS properties calculated at the UMP62X/6-31+G(d,p) level were very similar.
(43) De Meijere, A. *Angew. Chem., Int. Ed. Engl.* **1979**, *18*, 809−826.
(44) Hioe, J.; Zipse, H. Radical Stability—Thermochemical Aspects. In *Encyclopedia of Radicals in Chemistry, Biology and Materials*; Chatgilialoglu, C., Studer, A., Eds.; Wiley, 2012; Vol. *1*, *Basic Concepts and Methodologies*; http://onlinelibrary.wiley.com/book/10.1002/9781119953678.rad012.
(45) An MM2 computation with 2,2,3-trimethyl-1,2-oxasilolane and 2,2-dimethyl-1,2-oxasilinane models gave 3.5 kcal $mol^{-1}$ energy difference and a DFT [RB3LYP/6-311+G(2d,p)] computation indicated a 4.5 kcal $mol^{-1}$ difference.
(46) Luft, J. A. R.; Winkler, T.; Kessabi, F. M.; Houk, K. N. *J. Org. Chem.* **2008**, *73*, 8175−8181.


DOI: 10.1021/acs.joc.7b01011
*J. Org. Chem.* 2017, 82, 6886−6894